Nano-sulforaphane attenuates PhIP-induced early abnormal embryonic neuro-development

Ping Zhang[1,2#], Tingting Li[1,2#], Chang Liu[1,2#], Mustafa Sindi[3], Xin Cheng[1], Shuangyu Qi[1], Xinyue Liu[1], Yu Yan[1,2], Yongping Bao[4], Beate Brand-Saberi[3], Weidong Yang[5], Guang Wang[1,2*], Xuesong Yang[1,2*]

[1]*International Joint Laboratory for Embryonic Development & Prenatal Medicine, Division of Histology and Embryology, Medical College, Jinan University, Guangzhou 510632, China*

[2]*Key Laboratory for Regenerative Medicine of the Ministry of Education, Jinan University, Guangzhou 510632, China*

[3]*Department of Anatomy and Molecular Embryology, Institute of Anatomy, Ruhr University Bochum, Universitätsstrasse 150, 44801 Bochum, Germany.*

[4]*Norwich Medical School, University of East Anglia, Norwich, Norfolk NR4 7UQ, U.K.*

[5]*College of Life Science and Technology, Jinan University, Guangzhou, 510632, China.*

[#]*contributed to the work equally*

Running title: *Nano-SFN protects neurodevelopment*

[*]*The corresponding authors：Xuesong Yang Tel: +86-20-85228316. E-mail address: yang_xuesong@126.com or Guang Wang Tel: +86-20-85222054. E-mail address: t_wangguang@jnu.edu.cn, wangguang7453@126.com*

Abstract

Background

2-amino-1-methyl-6-phenylimidazo[4,5-b]pyrimidine (PhIP), one of the most abundant heterocyclic aromatic amines (HAA) formed by cooking meat at high temperatures, may modify humans and rodents through the metabolic process prior to affecting nervous system development. in humans and rodents may be modified by metabolic processes and then affecting nervous system development.

Methods

In this paper, PhIP was used to prepare a chicken embryo model with abnormal embryonic nervous system defects. Sulforaphane (SFN) is a derivative of a glucosinolate, which is abundant in cruciferous vegetables, and can pass through the placental barrier. Moreover, SFN has antioxidant and anti-apoptotic functions and is considered as a bioactive antioxidant with significant neuroprotective effects. Nano-sulforaphane (Nano-SFN, Sulforaphane nanoparticles) was prepared by self-assembly using biocompatible, biodegradable methoxy polyethylene glycol 5000-b-polyglutamic acid 10000 (mPEG5K-PGA10K) as the substrate, to explore the new application of Nano-SFN and its modified compounds as leading compounds in protecting against the abnormal development of the embryonic nervous system.

Results

The results show that Nano-SFN could protect against PhIP-induced central nervous system (CNS, derived from neural tube) and peripheral nervous system (PNS, derived from neural crest cells, NCCs) defects and neural tube defects (NTDs), and

increase the embryo survival rate.

Conclusions

This study indicates that Nano-SFN can effectively alleviate the developmental defects of embryonic nervous system induced by PhIP in the microenvironment and has a protective effect on embryonic development. It not only helps with expanding the application of SFN and improving its medicinal value, but also provides a possibility of SFN being developed as a novel drug for neuroprotection.

Keywords: 2-amino-1-methyl-6-phenylimidazo[4,5-b]pyridine; Sulforaphane nanoparticles; Embryonic development; Neural tube; Neural crest cells

1. Introduction

Birth defects or congenital anomalies include all structural and functional alterations in embryonic or fetal development resulting from genetic, environmental or unknown causes. Risk factors include advanced maternal and paternal ages, parental consanguinity and exposure to teratogenic agents (Oliveira et al., 2011). Congenital disease of the nervous system is the main type of birth defect (Mumpe-Mwanja et al., 2019). The nervous system includes the CNS and PNS, which are derived from the neural tube and NCCs of the embryo (Lukacs et al., 2019; Wilson et al., 2004). The neural system is one of the earliest systems to begin developing, during the 1st–8th weeks of embryonic development (teratogenic

sensitive period). Embryonic cells move and combine to form the primordia of organs, which are especially sensitive to teratogenic factors (Hill, 2007; Sadler, 2017).

Common teratogenic factors related to the development of the nervous system, such as alcohol consumption and smoking, have attracted wide attention (de la Monte et al., 2014; Meng et al., 2018), while teratogenic factors such as PhIP, identified as the most abundant heterocyclic amine produced in common cooking procedures (Keum et al., 2005), can affect early embryonic development, leading to abnormal development of the nervous system (Cruz-Hernandez et al., 2018; Griggs et al., 2014). Conventional toxicological studies of PhIP have focused on DNA damage (Bellamri et al., 2018; Hoelzl et al., 2008), carcinogenesis and oxidative damage (Griggs et al., 2014; Klewicka et al., 2012). However, exposure to PhIP during pregnancy and nursing may result in transference to fetuses and infants, plus, may be a critical risk factor for the generation of mammary carcinomas (Brittebo et al., 1994; Hasegawa et al., 1995). Knowledge on the toxicity of PhIP to the early neural system and candidate drugs to prevent it is still limited.

SFN is a dietary phytochemical that is abundant in cruciferous plants (Keum et al., 2005). It is regarded as a food, dietary supplement or medicine with low toxicity and is well tolerated by humans (Fahey et al., 2013; Fahey et al., 2012). SFN can protect cells from DNA damage (Russo et al., 2018) and is a potent antioxidant (Negrette-Guzman, 2019; Negrette-Guzman et al., 2013), which inhibits oxidative damage caused by various factors in neurons, glial cells, microglia and astrocytes (Danilov et al., 2009; Greco et al., 2010; Hong et al., 2005; Innamorato et al., 2008;

Kraft et al., 2004; Soriano et al., 2008). In our previous study, we found that 5–10μM SFN significantly rescued ethanol-suppressed angiogenesis in chick embryos (G. Wang et al., 2018). Nano-sized medicine, in comparison with conventional medicine, leads to increased active concentrations and bioavailability (Balakumar et al., 2013). Nano-SFN could be prepared by a self-assembly method using biocompatible, biodegradable methoxy polyethylene glycol 5000-b-polyglutamic acid 10000 (mPEG5K-PGA10K) as the substrate (Jiang et al., 2018; Xiao et al., 2013; Yang et al., 2019; Zhang et al., 2016). Thus, it was worth determining whether or not Nano-SFN could be a candidate drug for protection against the PhIP-induced abnormal development of the nervous system.

Both PhIP and nanoparticles can cross the placental barrier and enter the fetus from the external environment (Keum et al., 2005; Muoth et al., 2016). Therefore, we employed the chick embryo to investigate the neurodevelopmental toxicity of PhIP and the protective effects of Nano-SFN in this model induced by a PhIP microenvironment. The purpose was to develop a new type of Nano-SFN for the protection of embryonic development, which would not only expand the application of SFN and improves its practical value but also assist with the development of novel drugs, for example, for those with Nano-SFN as leading compounds. Through structural modification or reconstruction, it is expected to be possible to further increase its bioactivity or reduce its side effects.

2. Materials and methods

2.1. Preparation of Nano-SFN

Based on previous work in this field (Jiang et al., 2018; Xiao et al., 2013; Yang et al., 2019; Zhang et al., 2016), here, we describe for the first time the process of the encapsulation of 10μg/μl SFN into 0.05μg/μl mPEG5K-PGA10K by self-assembly. The SFN and mPEG5K-PGA10K were dissolved in pure dimethyl sulfoxide (DMSO) and sodium lactate Ringer's solution (LR), respectively. After 10 minutes, mPEG5K-PGA10K was gently dropped into the SFN–DMSO solution on a magnetic stirrer to ensure the supersaturation of the SFN solution. Then, the mixture was ultrasonicated for 30 minutes to accelerate the intermolecular interactions, and the solution was placed in a dark room at 4 °C overnight. Next, the solution was super-centrifuged for 20 minutes at 21380g, the supernatant was removed, and the precipitate was washed with LR; this step was repeated 5 times. Afterwards, the mixture was treated with ultrasound for 30 minutes to immobilize the molecular interactions (Figure 1). The content of free drugs in the supernatant was determined by high performance liquid chromatography (HPLC), and the drug encapsulation efficiency was 23.02% ± 2.7%.

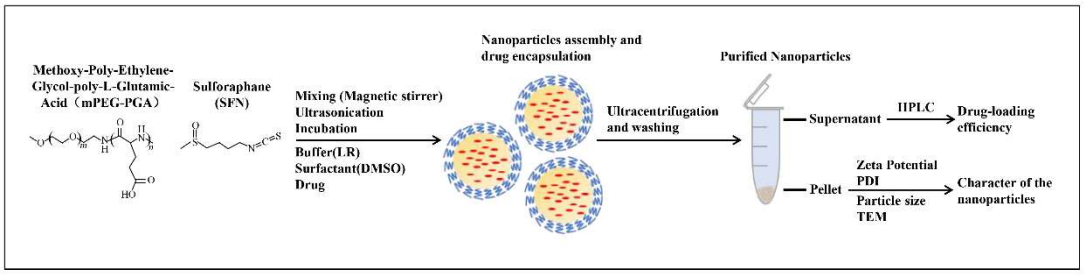

Figure 1 Schematic representation of the procedure of Nano-SFN synthesis.

2.2. Characterization of Nano-SFN

The SFN was purchased from Sigma (142825-10-3). mPEG5K-PGA10K was purchased from Xi'an Ruixi Biotechnology Co., Ltd. (R-PL1236-15K). SFN was packaged into mPEG5K-PGA10K by self-assembly to make Nano-SFN with a concentration of 5μM. The effective Nano-SFN dimensions and their size distributions were measured using a transmission electron microscope (TEM; TECNA12, FEI, USA). Additionally, the zeta potential of the Nano-SFN in Milli-Q water was determined by dynamic light scattering (DLS) using the Zetasizer Nano ZS instrument (Malvern Instruments Ltd, UK).

2.3. The zeta potential analyzer

The zeta potential of the Nano-SFN was determined by dynamic light scattering (DLS) using the Zetasizer Nano ZS instrument (Malvern Instruments Ltd, UK). The zeta potential analyzer was used to determine the nanoscale characteristics of the Nano-SFN, and the particle size distribution of the diluted nanoparticles was analyzed with a laser particle size distribution analyzer.

2.4. Early chick (EC) culture

Fertilized leghorn eggs were acquired from the Avian Farm of South China Agricultural University (Guangzhou, China). The fertilized eggs were incubated in a humidified incubator (Yiheng Instruments, Shanghai, China) set at 38 °C and 70% humidity until the chick embryos reached the desired developmental stage.

The early chick (EC) culture (Chapman SC., 2001) method was adopted to cultivate early chicken embryos, and the chicken embryos were divided into a control group (0.1% DMSO), 20μM PhIP group, 100μM PhIP group, 200μM PhIP group, 300μM PhIP group and 200μM PhIP + 5μM Nano-SFN group (n = 100 per group). The embryos were cultured from HH0 stage and treated from the beginning of the culture with the drugs mixed in the medium.

2.5. Immunofluorescent staining

The chicken embryos were harvested after incubation and fixed in 4% PFA overnight at 4 °C. The embryos were blocked with 10% Normal Goat Serum (SB Cat. No. 0060-01) and incubated with the following primary antibodies at 4 °C overnight on a shaker: HNK-1 (1:500, Sigma, USA), PAX7 (1:100, DSHB, USA), AP2α (1:100, Cell Signaling Technology, USA), Phospho-Histone H3 (pHH3, 1:200, Cell Signaling Technology, USA), neurofilament (NF, 1:200, Invitrogen Antibodies, USA) and cleaved-Caspase3 (c-Caspase3, 1:200, Cell Signaling Technology, USA). After extensive rinsing in PBST (0.1% Tween-20), the embryos were incubated with the corresponding Alexa Fluor 555 or 488 secondary antibody (1:1000, Invitrogen, USA) at 4 °C overnight on a shaker. The embryos were later counterstained with DAPI (1:1000, Invitrogen, USA) at room temperature for 2 hours.

2.6. Fluorescence microscopy photographs

After immunofluorescent staining, the whole-mount embryos and the regions of

interest were photographed using a stereoscope fluorescence microscope (Olympus MVX10) with imaging software (Image-Pro Plus 7.0). The embryos were then sectioned into 10μm-thick slices using a cryostat microtome (Leica CM1900, Germany) and photographed using an epi-fluorescent microscope (Olympus IX51, Leica DM 4000B) at 200x or 400x magnification with the Olympus software package Leica CW4000 FISH.

2.7. Data analysis

We used Image-Pro Plus 7.0 to quantify the $HNK1^+$ area, measuring the $HNK1^+$ staining and cell migration; NF^+, c-$Caspase3^+$ and $pHH3^+$ cells were manually counted in the DAPI and NF or c-Caspase3 or pHH3 merged images. All the experimental data analyses and statistical charts were generated using the SPSS 13.0 statistical software. The results are presented as the mean values (Mean ± SEM). Statistical significance was assessed by one-way ANOVA and Tukey's multiple comparisons test. $P < 0.05$ was considered to be statistically significant.

3. Result

3.1. Characterization of Nano-SFN

The surface charges of nanomaterials play a very decisive role, especially in electrocatalysis. A zeta potential analyzer was used to determine the characteristics of the prepared Nano-SFN. At pH 7.4, Nano-SFN had a zeta potential (ZP) of −7.21 mV

± 1.3 mV and a polydispersity index (PDI) of 0.430 ± 0.095 (Figure 2A-B). The alternative nanoparticles were used to analyze their distribution using a laser particle size distribution measuring instrument, and the particle size was observed to be 195 ± 32 nm (Figure 2A-B). The morphological sizes of Nano-SFN were observed by TEM (Figure 2C), the figure showed a nearly spherical shape and uniformly distributed size for the SFN nanoparticles.

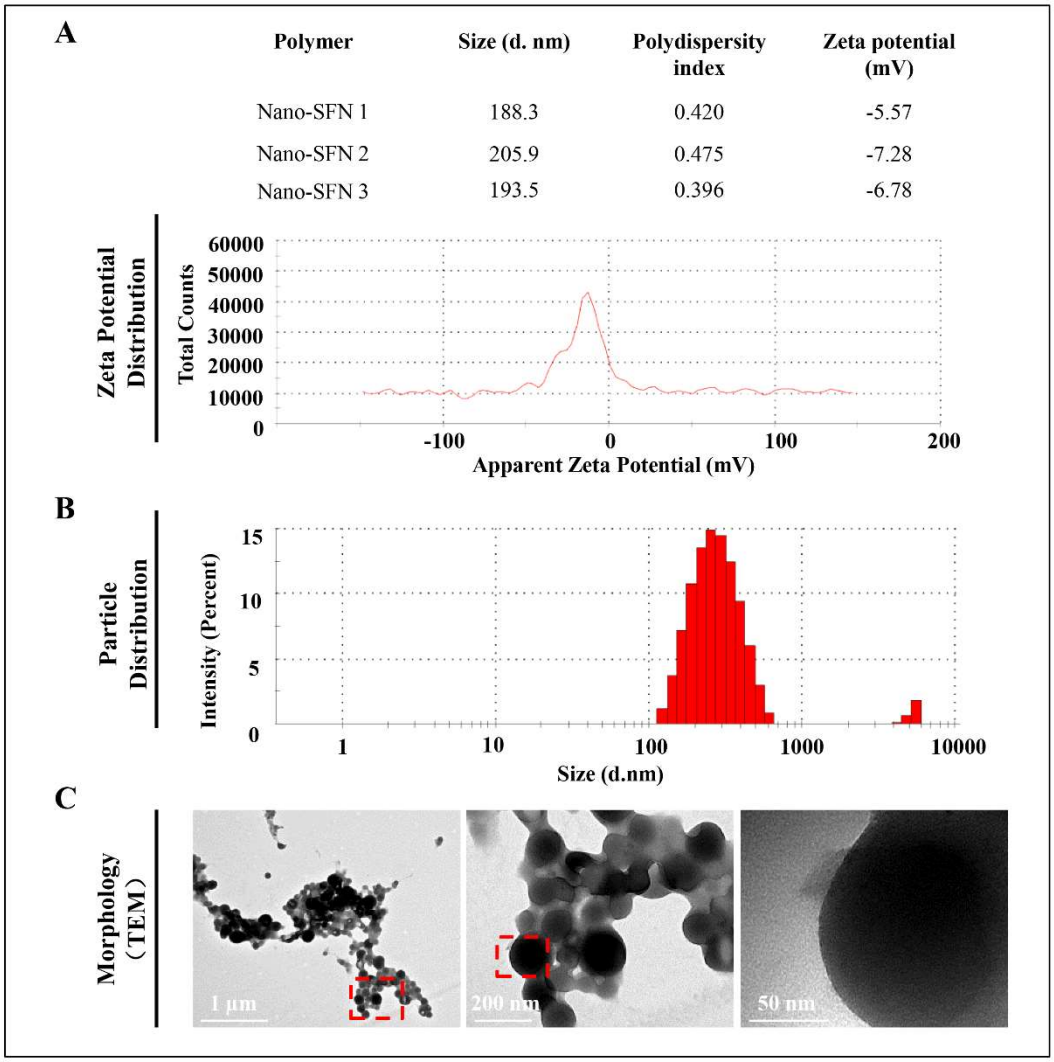

Figure 2 Nanoscale characterization of Nano-SFN. (A) The ZP and PDI of Nano-SFN were determined using a zeta potential analyzer. (B) Analysis of the particle size distribution of Nano-SFN using a laser particle size distribution

measuring instrument. d.nm: Diameter (nm) (C) TEM image of Nano-SFN; the scale bars are shown in the figure. Red dotted squares showed the enlarged regions of the left and middle TEM micrographs.

3.2. Nano-SFN reduced PhIP-induced embryonic death and NTDs

To investigate the effects of different experimental concentrations of PhIP on neurotoxicity and embryonic survival, chick embryos were first incubated with 0.1% DMSO (Control); 20μM, 100μM, 200μM, or 300μM PhIP; or 200μM PhIP + 5μM Nano-SFN for 36 h in early chick (EC) culture. The previously study showed that 0.1% DMSO did not affect the embryo development (Gao, L.R et al., 2016), we also tested the effects of the packaging materials (mPEG5K-PGA10K) on the development of chicken embryos, the results proved that there was no significant negative effect on the mortality and length of chick embryos (Supplementary Figure 1).

PAX7 expression is restricted to the dorsal half of the neural tube, as Figure 3A shows. The embryo could not grow normally, and there is no obvious fluorescence, indicating that they were dead embryos. While the normal embryos showed normal closure of the neural tube in the head and trunk, neural tube malformation could be observed in the PhIP-treated groups—the failure of neural tube closure—according to PAX7 immunofluorescence (Figure 3B, indicated by white arrow), the failure of neural tube closure is a severe birth defects of the CNS, namely NTDs. The mortality rates and neural tube malformation rates were increased in the PhIP-treated embryos in a dose-dependent manner and could be reversed by the Nano-SFN. The mortality

rates were 0% for the Control, 8% with 20μM PhIP, 20.17% with 100μM PhIP, 53.41% with 200μM PhIP, 85% with 300μM PhIP, and 7% with 200μM PhIP + 5μM Nano-SFN. The neural tube malformation rates were 0% for the Control, 5% with 20μM PhIP, 14.29% with 100μM PhIP, 35.80% with 200μM PhIP, 14% with 300μM PhIP, and 6% with 200μM PhIP + 5μM Nano-SFN (Figure 3C).

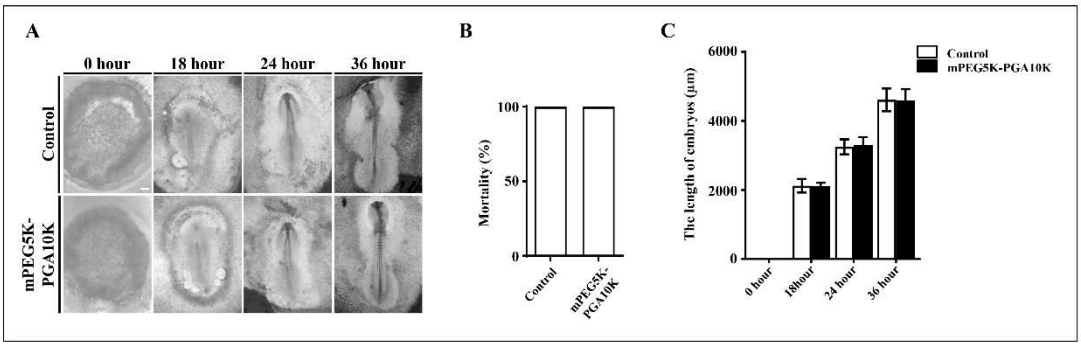

Supplementary Figure 1 The effects of MPEG5K-PGA10K on the developmental chicken embryos. (A) Representative images of chicken embryos which were treated in 0.1 % DMSO or MPEG5K-PGA10K for 0, 18, 24 and 36 hours (n = 10 per group). (B) Bar chart showing the mortality rates of chick embryos. (C) Bar chart showing the length of chick embryos for various time (hours). Scale bars = 400μm (A).

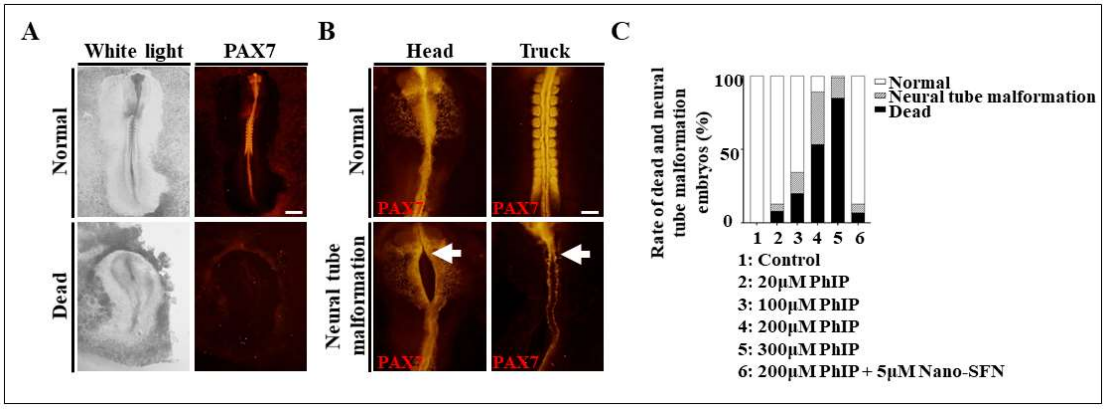

Figure 3 Nano-SFN reduced PhIP-induced embryonic death and NTDs. (A) Immunofluorescence of PAX7 in chicken embryos at stage HH10 in the different treatment groups (n = 10 per group). (B) Immunofluorescence of PAX7 in the heads

and trunks of the chick embryos. The white arrows indicate neural tube malformations and neural tube closure defects. (C) Bar chart showing the difference in the HH10 chicken embryo mortality and neural tube malformation rates among the different treatment groups. Scale bars = 500μm (A) and 200μm (B).

3.3. Nano-SFN efficiently reversed PhIP-inhibited neural cell differentiation in the neural tube

To investigate whether Nano-SFN played an active role in rescuing PhIP-induced suppression in neurogenesis, we implemented immunofluorescence staining with an NF antibody (Figure 4A). We observed that NF expression in the neural tubes (indicated by arrows) of the HH10 chick embryos was suppressed by 200μM PhIP but dramatically recovered after the administration of 5μM Nano-SFN (Control = 23.99 ± 5.21; 200μM PhIP = 4.85 ± 1.96; 200μM PhIP + 5μM Nano-SFN = 20.22 ± 7.22; Figure 4B). The experiment confirmed that in the chicken embryo model, the PhIP-induced inhibition of the neural cell differentiation of neural tube cells can be ameliorated by adding 5μM Nano-SFN.

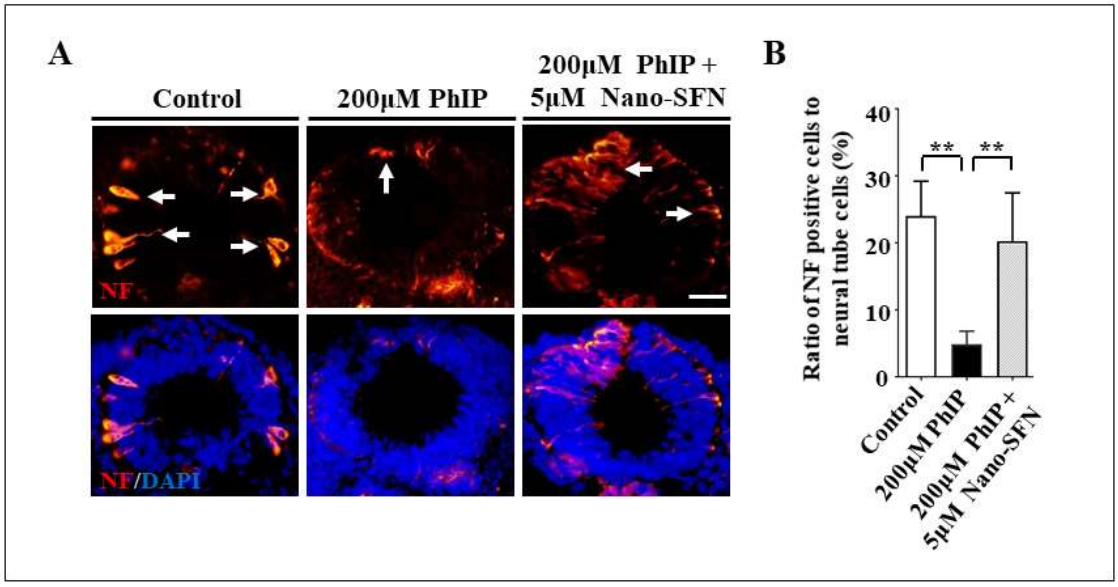

Figure 4 PhIP-induced inhibition of the neural cell differentiation of neural tube cells can be improved by adding Nano-SFN. (A) Immunofluorescence of NF in the neural cells of the chick embryos. White arrows indicate NF-positive cells (n = 12 per group). (B) Bar chart comparing the ratios of the positive neural cells among the different treatment groups. **p<0.01. Scale bars = 50μm (A).

3.4. Nano-SFN improved PhIP-suppressed NCCs generation and migration

Ap2α immunofluorescence was used to characterize cranial neural crest cells (CNCCs) (Figure 5A; the expression is represented by the white area, and the white arrows indicate the sections), and the effects in the control, 200μM PhIP and 200μM PhIP + 5μM Nano-SFN groups on the CNCCs in the chicken embryos were detected. The results showed that CNCCs were significantly decreased after the treatment with 200μM PhIP, and the production of CNCCs returned to normal after 5μM Nano-SFN treatment (Control = 9.31 ± 1.69; 200μM PhIP = 6.54 ± 1.97; 200μM PhIP + 5μM Nano-SFN = 9.42 ± 0.84; Figure 5B). In addition, according to the specific staining of

migrating NCCs with HNK1 (shown in the white area of Figure 5C), the HNK1 expression area was decreased significantly by treatment with 200μM PhIP, and the HNK1-positive area increased significantly after the 200μM PhIP + 5μM Nano-SFN treatment (Control = 8.59 ± 2.02; 200μM PhIP = 4.04 ± 3.45; 200μM PhIP + 5μM Nano-SFN = 8.27 ± 2.75; Figure 5D). The experiment confirmed that in the chicken embryo model, the inhibition of NCCs production and migration by PhIP can be improved by adding Nano-SFN.

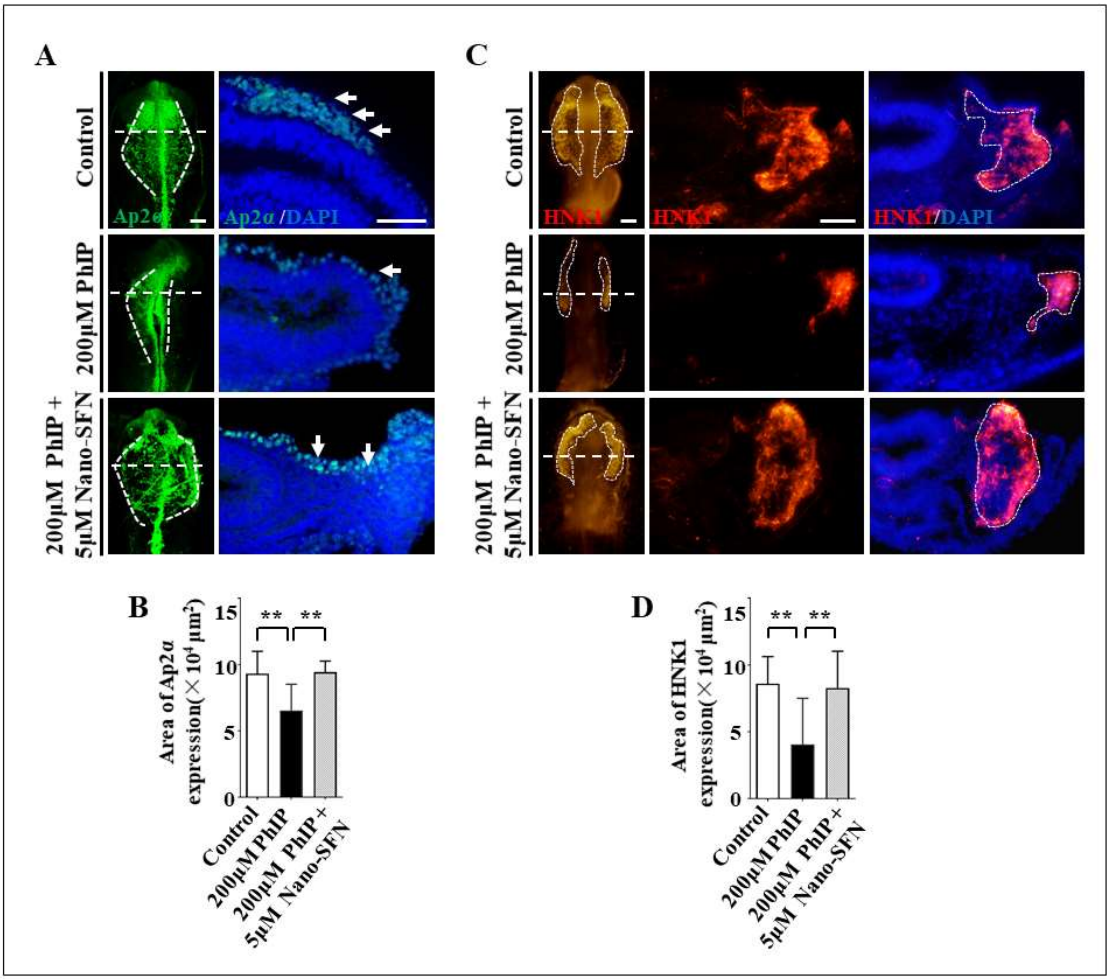

Figure 5 Nano-SFN can ameliorate the inhibition by PhIP of NCCs production and migration. (A) Whole-mount immunofluorescence and transverse sections of the Ap2α in CNCCs. (B) Bar chart comparing the CNCC areas among the different

treatment groups. (C) Representative images of migratory NCCs stained with HNK1 as indicated by the dotted squares. (D) Bar chart comparing migrating NCC areas among the different treatment groups. **p<0.01. Scale bars = 100μm (whole-mount); 50μm (section). n = 18 (B), 41 (D).

3.5. Nano-SFN ameliorated PhIP-induced neural tube cell apoptosis and inhibition of neural tube cell proliferation

We cultured chicken embryos to HH10 and labeled the proliferating cells on the neural tube with pHH3 (Figure 6A). The results showed that the number of pHH3-positive cells decreased significantly under 200μM PhIP treatment, while following 200μM PhIP + 5μM Nano-SFN treatment, the number of pHH3-positive cells returned to normal levels (Control = 13 ± 3.03; 200μM PhIP = 5.07 ± 1.77; 200μM PhIP + 5μM Nano-SFN = 12.71 ± 2.69; Figure 6B). At the same time, apoptotic cells in the neural tube were labelled with c-Caspase3 (Figure 6C), which showed that the number of c-Caspase3-positive cells increased significantly under 200μM PhIP treatment. By contrast, the number of c-Caspase3-positive cells decreased significantly under 200μM PhIP + 5μM Nano-SFN treatment (Control = 6.14 ± 1.95; 200μM PhIP = 18.46 ± 5.62; 200μM PhIP + 5μM Nano-SFN = 7.00 ± 2.38; Figure 6D). The experiments confirmed that Nano-SFN could significantly ameliorate PhIP-induced neural tube cell apoptosis and inhibition of neural tube cell proliferation in the chicken embryo model.

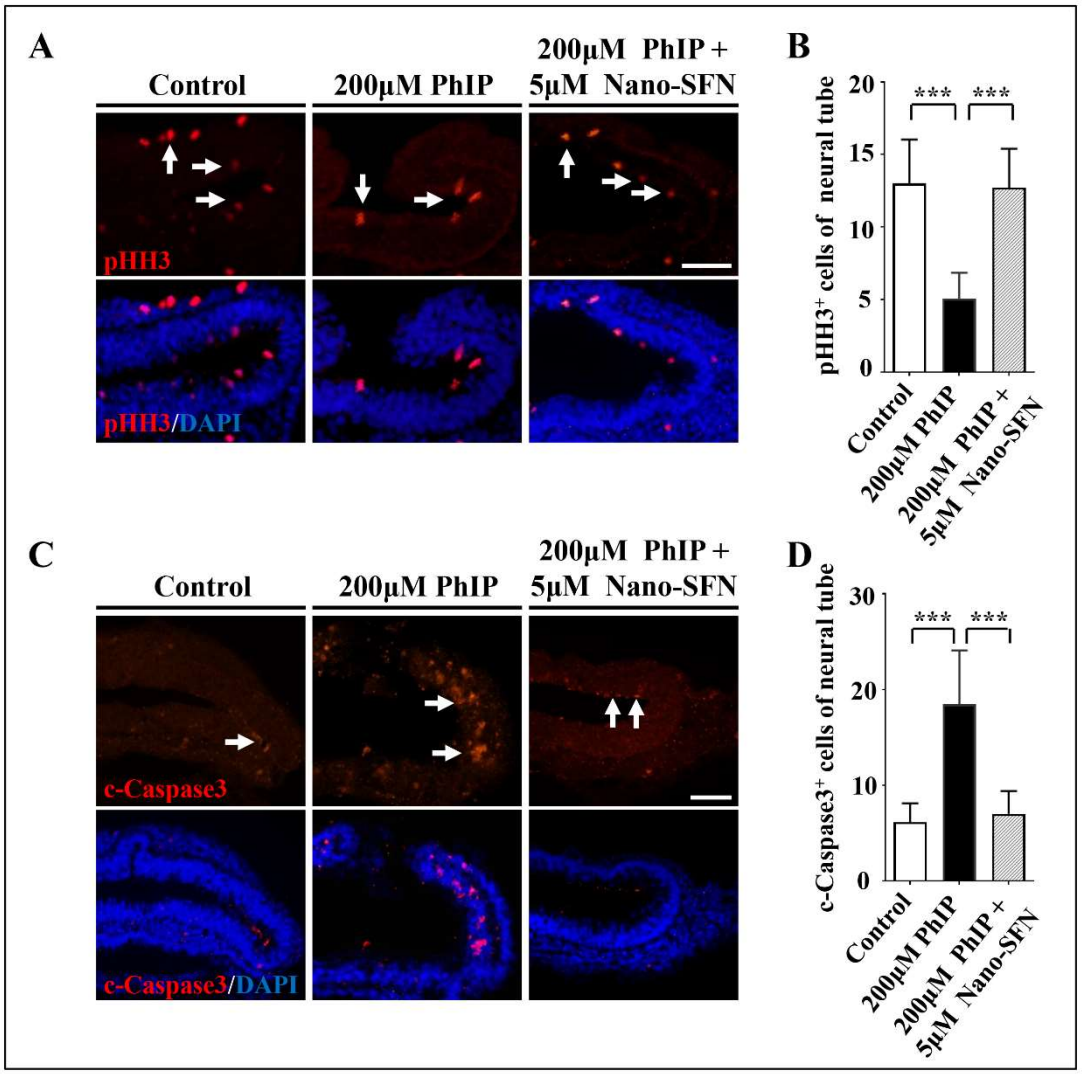

Figure 6 Nano-SFN ameliorated PhIP-induced apoptosis and inhibition of the proliferation of embryonic neural tube cells. (A) The merged images from the pHH_3^+ and DAPI staining of the chick embryo neural tubes, with pHH_3^+ cells indicated by the white arrows. (B) Bar chart comparing the proliferating cell areas from the chick embryo neural tube among the different treatment groups. (C) Representative images of chick embryo neural tube apoptotic cells stained with c-Caspase3 as indicated by the white arrows. (D) Bar chart comparing the apoptotic cell areas among the different treatment groups. ***$p<0.001$. n = 27 per group (B) and (D). Scale bar = 50μm (A) and (C).

4. Discussion

A number of recent studies have demonstrated great potential of nanotechnology in the diagnosis and treatment of various human diseases in biomedicine (Kinnear et al., 2017). Meanwhile, there're many articles indicating that biological nanotechnology is one of the most intruiging fields in nanoscience applications. In recent decades, the applications of nanotechnology in a number of biology-related fields—such as diagnostics, drug delivery and molecular imaging—have been thoroughly researched, with excellent results. However, the most significant advances in nanotechnology belong to the field of biomedicine, in which they possess a huge potential to provide innovative solutions. With the advancement of modern science, it is becoming more and more feasible to design targeted or multifunctional nanotechnology products for therapeutic applications. There are many parameters that are important for the successful development and manufacture of targeted drug delivery vehicles. The efficacy of nanoparticles as a vehicle is highly dependent on both size and shape (Navya, P.N., 2019). The size of the nanoparticles affects their movement into and out of the blood vessels, and the particle at the edge of the blood vessel wall is affected by its shape (Farokhzad et al., 2009). As shown in the figure, the Nano-SFN we made are nearly spherical, with a uniform particle size; the particle size is 195 ± 32 nm, and the particle distribution is relatively uniform (Figure 2). Therefore, Nano-SFN prepared by our method could easily enter and exit blood vessels, as well as pass through the placental barrier and be suitable for absorption in the human body.

Neural development involves a series of coordinated morphological events that cause the flat nerve plate to turn into a neural tube, the primordium base of the entire CNS (Copp et al., 2003). NTDs can lead to severe abnormalities of the CNS, which are one of the most common congenital malformations in humans (Sanna et al., 2019). PhIP has been shown to have a negative effect on early embryonic development. In this study, the effect of PhIP's experimental concentration on neurotoxicity and the embryo survival rate was studied. Embryo mortality in the experimental groups of our study was the highest in the 200μM PhIP group in terms of the median lethal dose (LD50) and neural tube malformation rates. Therefore, 200μM PhIP was selected for the treatment group, and a 5μM Nano-SFN intervention was chosen based on existing literature (G. Wang et al., 2018). The results showed that Nano-SFN reduced PhIP-induced embryonic death and NTDs.

Neural tube closure has been studied for many decades. We can easily observe the NTDs using the Pax7 immunofluorescence (Figure 3). However, Pax7 does have systemic expression on embryos including neural tube and somites. The malformation of somites also can be found, which suggested that PhIP on embryonic development in general. In this study, our research only focused on neurogenesis because neurogenesis is one of the earliest processes that occur in embryonic development. NTDs is complex and involves cellular events. Proper differentiation, cell survival and neural crest migration are closely related to neural tube development (Nikolopoulou et al., 2017). Neurons can be determined by the NF protein (Regan, 1988). We found that the PhIP-induced inhibition of the neural cell differentiation of

neural tube cells could be reversed by adding 5μM Nano-SFN (Figure 4). The development of the nervous system is a complex process involving the induction, determination and movement of cells. NCCs are a pluripotent cell group with high migrative ability. The signaling of PNS elements is mediated by specific cell groups that originate from the top of the neural tube—that is, NCCs (Catala et al., 2013)—and in the process of development, NCCs migrate normally to form the neurons and glial cells of the PNS, which are of great significance to the establishment of the embryonic nervous system (Giovannone et al., 2015). In our study, the application of AP2α (specifically expressed on CNCCs) and HNK-1 (expressed on migrating NCCs) (Minarcik et al., 2003) allowed us to reveal that pre-migratory and migrating CNCCs were significantly affected by PhIP, and the addition of Nano-SFN could ameliorate the inhibition of NCCs production and migration by PhIP (Figure 5).

Neurogenesis plays a key role in the neuroplasticity of the CNS, brain homeostasis and maintenance (Poulose et al., 2017); this process is a highly complex, multi-step process that begins with the proliferation of progenitor cells (Balu et al., 2009). Orderly cell apoptosis also regulates normal processes in embryogenesis such as the fusion of the oral palate and neural tube and craniofacial development (Graham et al., 1993; Graham et al., 1996; Lawson et al., 1998; Weil et al., 1997). However, teratogenic factor-induced excess apoptosis is always involved in NTDs and NCCs developmental anomalies (Chappell et al., 2009; Torchinsky et al., 2005). In this paper, pHH_3 and c-Caspase3 were used to label proliferating cells and apoptotic cells in the

neural tube (Figure 6). Apoptosis is one of several integrated responses to DNA damage (J. Y. Wang, 2001). Nano-SFN might target PhIP-induced excessive DNA damage, which may, in turn, contributing to the protective effects on embryonic neurogenesis.

This article mainly discusses the new application of Nano-SFN in the protection against embryonic nervous system dysplasia. The results show that Nano-SFN plays an important role in the formation of the CNS and PNS in the embryonic nervous system, indicating that Nano-SFN can effectively alleviate the PhIP microenvironment-induced abnormal development of the embryonic nervous system and has a protective effect on embryonic development. Based on our findings, the women at the early stage of pregnancy should avoid taking barbecue, instead, increase intake amount of cruciferous vegetables, which benefits the fetal neural development. The range of applications for SFN has been expanded, and the practical value of SFN has been improved, which provides the possibility of further developing new drugs.

Acknowledgements

This study was supported by NSFC grant (31971108, 31771331), Science and Technology Planning Project of Guangdong Province (2017A020214015, 2017A050506029), Science and Technology Program of Guangzhou (201710010054), The Training Program for Undergraduate (201910559091, CX2019107, CX2019101, 19112032). We thank Dr. Christopher Dacosta (MDPI, Manchester UK) for carefully reading this manuscript, and helpful discussions.

Author contributions

All authors contributed to the study conception and design. Xuesong Yang: Conceptualization, Investigation, Methodology, Project administration; Guang Wang: Software, Formal analysis, Supervision, Writing - review & editing; Ping Zhang: Investigation, Formal analysis, Writing - original draft; Tingting Li: Visualization, Data curation, Writing - original draft; Chang Liu: Resources, Investigation, Validation; Mustafa Sindi: Material preparation, Resources; Xin Cheng: Supervision, Writing - review & editing; Shuangyu Qi: Investigation, Validation; Xinyue Liu: Investigation, Tissue collection; Yu Yan: Investigation, Validation; Yongping Bao: Writing - review & editing; Weidong Yang: Methodology; Beate Brand Saberi: Writing - review & editing.

Ethical statement

All animal protocols were approved by the Jinan University Laboratory Animal Committee on Animal Welfare (IACUC-20181126-02).

Competing interests

The authors declare that there are no competing financial interests.

References

Oliveira, C. I., Richieri-Costa, A., Carvalho Ferrarese, V. C., Moz Vaz, D. C., Fett-Conte, A. C. (2011). Birth defects in newborns and stillborns: an example of the Brazilian reality.

BMC Res Notes, 4, 343.
Mumpe-Mwanja, D., Barlow-Mosha, L., Williamson, D., Valencia, D., Serunjogi, R., Kakande, A., et al. (2019). A hospital-based birth defects surveillance system in Kampala, Uganda. BMC Pregnancy Childbirth, 19(1), 372.
Lukacs, M., Roberts, T., Chatuverdi, P., Stottmann, R. W. (2019). Glycosylphosphatidylinositol biosynthesis and remodeling are required for neural tube closure, heart development, and cranial neural crest cell survival. Elife, 8.
Wilson, Y. M., Richards, K. L., Ford-Perriss, M. L., Panthier, J. J., Murphy, M. (2004). Neural crest cell lineage segregation in the mouse neural tube. Development, 131(24), 6153-6162.
Hill, M. A. (2007). Early human development. Clin Obstet Gynecol, 50(1), 2-9.
Sadler, T. W. (2017). Establishing the Embryonic Axes: Prime Time for Teratogenic Insults. J Cardiovasc Dev Dis, 4(3).
de la Monte, S. M., Kril, J. J. (2014). Human alcohol-related neuropathology. Acta Neuropathol, 127(1), 71-90.
Meng, X., Sun, Y., Duan, W., Jia, C. (2018). Meta-analysis of the association of maternal smoking and passive smoking during pregnancy with neural tube defects. Int J Gynaecol Obstet, 140(1), 18-25.
Keum, Y. S., Jeong, W. S., Kong, A. N. (2005). Chemopreventive functions of isothiocyanates. Drug News Perspect, 18(7), 445-451.
Cruz-Hernandez, A., Agim, Z. S., Montenegro, P. C., McCabe, G. P., Rochet, J. C., Cannon, J. R. (2018). Selective dopaminergic neurotoxicity of three heterocyclic amine subclasses in primary rat midbrain neurons. Neurotoxicology, 65, 68-84.
Griggs, A. M., Agim, Z. S., Mishra, V. R., Tambe, M. A., Director-Myska, A. E., Turteltaub, K. W., et al. (2014). 2-Amino-1-methyl-6-phenylimidazo[4,5-b]pyridine (PhIP) is selectively toxic to primary dopaminergic neurons in vitro. Toxicol Sci, 140(1), 179-189.
Bellamri, M., Wang, Y., Yonemori, K., White, K. K., Wilkens, L. R., Le Marchand, L., et al. (2018). Biomonitoring an albumin adduct of the cooked meat carcinogen 2-amino-1-methyl-6-phenylimidazo[4,5-b]pyridine in humans. Carcinogenesis, 39(12), 1455-1462.
Hoelzl, C., Glatt, H., Meinl, W., Sontag, G., Haidinger, G., Kundi, M., et al. (2008). Consumption of Brussels sprouts protects peripheral human lymphocytes against 2-amino-1-methyl-6-phenylimidazo[4,5-b]pyridine (PhIP) and oxidative DNA-damage: results of a controlled human intervention trial. Mol Nutr Food Res, 52(3), 330-341.
Klewicka, E., Nowak, A., Zdunczyk, Z., Juskiewicz, J., Cukrowska, B. (2012). Protective effect of lactofermented red beetroot juice against aberrant crypt foci formation, genotoxicity of fecal water and oxidative stress induced by 2-amino-1-methyl-6-phenylimidazo[4,5-b] pyridine in rats model. Environ Toxicol Pharmacol, 34(3), 895-904.
Brittebo, E. B., Karlsson, A. A., Skog, K. I., Jagerstad, I. M. (1994). Transfer of the food mutagen PhIP to foetuses and newborn mice following maternal exposure. Food Chem Toxicol, 32(8), 717-726.

Hasegawa, R., Kimura, J., Yaono, M., Takahashi, S., Kato, T., Futakuchi, M., et al. (1995). Increased risk of mammary carcinoma development following transplacental and trans-breast milk exposure to a food-derived carcinogen, 2-amino-1-methyl-6-phenylimidazo[4,5-b]pyridine (PhIP), in Sprague-Dawley rats. Cancer Res, 55(19), 4333-4338.

Fahey, J. W., Kensler, T. W. (2013). Health span extension through green chemoprevention. Virtual Mentor, 15(4), 311-318.

Fahey, J. W., Talalay, P., Kensler, T. W. (2012). Notes from the field: "green" chemoprevention as frugal medicine. Cancer Prev Res (Phila), 5(2), 179-188.

Russo, M., Spagnuolo, C., Russo, G. L., Skalicka-Wozniak, K., Daglia, M., Sobarzo-Sanchez, E., et al. (2018). Nrf2 targeting by sulforaphane: A potential therapy for cancer treatment. Crit Rev Food Sci Nutr, 58(8), 1391-1405.

Negrette-Guzman, M. (2019). Combinations of the antioxidants sulforaphane or curcumin and the conventional antineoplastics cisplatin or doxorubicin as prospects for anticancer chemotherapy. Eur J Pharmacol, 859, 172513.

Negrette-Guzman, M., Huerta-Yepez, S., Tapia, E., Pedraza-Chaverri, J. (2013). Modulation of mitochondrial functions by the indirect antioxidant sulforaphane: a seemingly contradictory dual role and an integrative hypothesis. Free Radic Biol Med, 65, 1078-1089.

Danilov, C. A., Chandrasekaran, K., Racz, J., Soane, L., Zielke, C., Fiskum, G. (2009). Sulforaphane protects astrocytes against oxidative stress and delayed death caused by oxygen and glucose deprivation. Glia, 57(6), 645-656.

Greco, T., Fiskum, G. (2010). Brain mitochondria from rats treated with sulforaphane are resistant to redox-regulated permeability transition. J Bioenerg Biomembr, 42(6), 491-497.

Hong, F., Freeman, M. L., Liebler, D. C. (2005). Identification of sensor cysteines in human Keap1 modified by the cancer chemopreventive agent sulforaphane. Chem Res Toxicol, 18(12), 1917-1926.

Innamorato, N. G., Rojo, A. I., Garcia-Yague, A. J., Yamamoto, M., de Ceballos, M. L., Cuadrado, A. (2008). The transcription factor Nrf2 is a therapeutic target against brain inflammation. J Immunol, 181(1), 680-689.

Kraft, A. D., Johnson, D. A., Johnson, J. A. (2004). Nuclear factor E2-related factor 2-dependent antioxidant response element activation by tert-butylhydroquinone and sulforaphane occurring preferentially in astrocytes conditions neurons against oxidative insult. J Neurosci, 24(5), 1101-1112.

Soriano, F. X., Leveille, F., Papadia, S., Higgins, L. G., Varley, J., Baxter, P., et al. (2008). Induction of sulfiredoxin expression and reduction of peroxiredoxin hyperoxidation by the neuroprotective Nrf2 activator 3H-1,2-dithiole-3-thione. J Neurochem, 107(2), 533-543.

Wang, G., Nie, J.-h., Bao, Y., Yang, X. (2018). Sulforaphane Rescues Ethanol-Suppressed Angiogenesis through Oxidative and Endoplasmic Reticulum Stress in Chick Embryos. Journal of Agricultural and Food Chemistry, 66(36), 9522-9533.

Balakumar, K., Raghavan, C. V., selvan, N. T., prasad, R. H., Abdu, S. (2013). Self nanoemulsifying drug delivery system (SNEDDS) of rosuvastatin calcium: design,

formulation, bioavailability and pharmacokinetic evaluation. Colloids Surf B Biointerfaces, 112, 337-343.
Jiang, Y., Fay, J. M., Poon, C. D., Vinod, N., Zhao, Y., Bullock, K., et al. (2018). Nanoformulation of Brain-Derived Neurotrophic Factor with Target Receptor-Triggered-Release in the Central Nervous System. Adv Funct Mater, 28(6).
Xiao, H., Stefanick, J. F., Jia, X., Jing, X., Kiziltepe, T., Zhang, Y., et al. (2013). Micellar nanoparticle formation via electrostatic interactions for delivering multinuclear platinum(II) drugs. Chem Commun (Camb), 49(42), 4809-4811.
Yang, X., Yu, Y., Huang, X., Chen, Q., Wu, H., Wang, R., et al. (2019). Delivery of platinum (II) drugs with bulky ligands in trans-geometry for overcoming cisplatin drug resistance. Mater Sci Eng C Mater Biol Appl, 96, 96-104.
Zhang, L., Zhang, P., Zhao, Q., Zhang, Y., Cao, L., Luan, Y. (2016). Doxorubicin-loaded polypeptide nanorods based on electrostatic interactions for cancer therapy. J Colloid Interface Sci, 464, 126-136.
Muoth, C., Aengenheister, L., Kucki, M., Wick, P., Buerki-Thurnherr, T. (2016). Nanoparticle transport across the placental barrier: pushing the field forward! Nanomedicine (Lond), 11(8), 941-957.
Gao, L.R., Li, S., Zhang, J., et al. (2016). Excess Imidacloprid Exposure Causes the Heart Tube Malformation of Chick Embryos. J Agric Food Chem, 64(47), 9078-9088.
Chapman, S. C., Collignon, J., Schoenwolf, G. C., Lumsden, A. (2001). Improved method for chick whole-embryo culture using a filter paper carrier. Dev Dyn, 220(3), 284-289.
Kinnear, C., Moore, T. L., Rodriguez-Lorenzo, L., Rothen-Rutishauser, B., Petri-Fink, A. (2017). Form Follows Function: Nanoparticle Shape and Its Implications for Nanomedicine. Chemical Reviews, 117(17), 11476-11521.
Navya, P.N., Kaphle, A., Srinivas, S.P. et al. (2019). Current trends and challenges in cancer management and therapy using designer nanomaterials. Nano Convergence, 6(1), 23.
Farokhzad, O. C., Langer, R. (2009). Impact of nanotechnology on drug delivery. ACS Nano, 3(1), 16-20.
Copp, A. J., Greene, N. D., Murdoch, J. N. (2003). The genetic basis of mammalian neurulation. Nat Rev Genet, 4(10), 784-793.
Sanna, S., van Zuydam, N. R., Mahajan, A., Kurilshikov, A., Vich Vila, A., Vosa, U., et al. (2019). Causal relationships among the gut microbiome, short-chain fatty acids and metabolic diseases. Nat Genet, 51(4), 600-605.
Nikolopoulou, E., Galea, G. L., Rolo, A., Greene, N. D., Copp, A. J. (2017). Neural tube closure: cellular, molecular and biomechanical mechanisms. Development, 144(4), 552-566.
Regan, C. M. (1988). Neuronal and glial markers of the central nervous system. Experientia, 44(8), 695-697.
Catala, M., Kubis, N. (2013). Gross anatomy and development of the peripheral nervous system. Handb Clin Neurol, 115, 29-41.
Giovannone, D., Ortega, B., Reyes, M., El-Ghali, N., Rabadi, M., Sao, S., et al. (2015). Chicken trunk neural crest migration visualized with HNK1. Acta Histochem, 117(3), 255-266.
Minarcik, J. C., Golden, J. A. (2003). AP-2 and HNK-1 define distinct populations of cranial

neural crest cells. Orthod Craniofac Res, 6(4), 210-219.
Poulose, S. M., Miller, M. G., Scott, T., Shukitt-Hale, B. (2017). Nutritional Factors Affecting Adult Neurogenesis and Cognitive Function. Adv Nutr, 8(6), 804-811.
Balu, D. T., Lucki, I. (2009). Adult hippocampal neurogenesis: regulation, functional implications, and contribution to disease pathology. Neurosci Biobehav Rev, 33(3), 232-252.
Graham, A., Heyman, I., Lumsden, A. (1993). Even-numbered rhombomeres control the apoptotic elimination of neural crest cells from odd-numbered rhombomeres in the chick hindbrain. Development, 119(1), 233-245.
Graham, A., Koentges, G., Lumsden, A. (1996). Neural crest apoptosis and the establishment of craniofacial pattern: an honorable death. Mol Cell Neurosci, 8(2-3), 76-83.
Lawson, A., England, M. A. (1998). Neural fold fusion in the cranial region of the chick embryo. Dev Dyn, 212(4), 473-481.
Weil, M., Jacobson, M. D., Raff, M. C. (1997). Is programmed cell death required for neural tube closure? Curr Biol, 7(4), 281-284.
Chappell, J. H., Jr., Wang, X. D., Loeken, M. R. (2009). Diabetes and apoptosis: neural crest cells and neural tube. Apoptosis, 14(12), 1472-1483.
Torchinsky, A., Fein, A., Toder, V. (2005). Teratogen-induced apoptotic cell death: does the apoptotic machinery act as a protector of embryos exposed to teratogens? Birth Defects Res C Embryo Today, 75(4), 353-361.
Wang, J. Y. (2001). DNA damage and apoptosis. Cell Death Differ, 8(11), 1047-1048.